Jonal of Mobile Multimedia, Vol. 7, No.4 (2011) 256-266

PERFORMANCE COMPARISON OF AIRBORNE PHASED-ARRAY AND MIMO RADAR WITH SUBARRAYS

YONGZHE LI HUIYONG LI JUN LI ZISHU HE

University of Electronic Science and Technology of China, China
lyzlyz888@gmail.com;hyli@uestc.edu.cn;lijun_sc@126.com;zshe@uestc.edu.cn

Received December 7, 2011
Revised April 10, 2012

A generalized signal model for airborne phased-array (PA) and multi-input multi-output (MIMO) radar with colocated antennas is proposed. This model is based on partitioning the transmit array into a certain number of uniform subarrays that are allowed to overlap. Different subarrays transmit identical waveforms for PA radar while orthogonal or non-coherent ones for MIMO which maintains coherent processing gain in each of them. Passive element-level phase shifting is utilized within each subarray in order to steer the scanning beams. On the basis of the unified model, we focus on the performances of space-time adaptive processing (STAP) and nonadaptive processing technique by formulating and evaluating the signal-to-interference-noise ratio (SINR) for PA and MIMO radar. Beamforming-based modified joint domain localized (BBM-JDL) method is employed as the STAP technique. It is verified that under the same coverage condition, performances of PA and uniform non-overlapped MIMO radar are nearly same, while fully overlapped MIMO radar possesses the potential of achieving higher performance.

Key words: Airborne MIMO radar, PA, Subarray, STAP, BBM-JDL

1 Introduction

In recent years, the study around multi-input multi-output (MIMO) radar has received increasing attention since the groundbreaking work was announced [1]. The concept "MIMO" is first used in communications to increase data throughput and link range without additional bandwidth or transmit power. In the context of radar, it simply means that there are multiple radiating and receiving sites. Unlike standard phased-array (PA) radar which transmits an identical waveform, a MIMO radar system can transmit multiple probing signals that can be orthogonal [1]-[5] or noncoherent [6]-[8]. In the review work edited by Li [9], it is shown that the added flexibility produced by waveform diversity brings with MIMO radar the promise of enormous performance improvements including significantly improved parameter identifiability, enhanced inflexibility for transmit beampattern design and better clutter mitigation performance.

At present, some efforts aiming at jointly combining phased-array (PA) and MIMO radar have been made [10], taking the point of view that MIMO radar is simply the next step in the evolution of PA radar system. Considering that the number of elements of modern phased-array system can be up to extremely large, the idea of dividing the aperture of transmit array with colocated antennas into

multiple disjoint subapertures becomes even more valuable. This enables us to directly apply the PA hardware without the need of specially antenna design for MIMO radar. However, it is challenging due to large computational complexity cost when conducting signal processing strategies. MIMO radar signal processing technology can be more complex than its counterpart because it has to properly deal with the extra filtered transmitting degrees of freedom (DOFs) at the receiving end. Thus different performances can be achieved for PA and MIMO radar.

In [11], a method for generating multiple correlated signals that could be used to drive individual transmitters is proposed, demonstrating that MIMO radar with subarrays possesses the potential to achieve arbitrary spatial beampatterns on transmitter while maintaining full PA resolution on receiver. In [12], the concept of phased-MIMO radar is used and several advantages are analyzed in terms of the corresponding beampattern and signal-to-interference-plus-noise ratio (SINR) expressions compared with its PA and MIMO counterparts.

In this paper, we extend this concept to airborne radar field in which clutter mitigation is of prime importance. When it comes to airborne radar application, space-time adaptive processing (STAP) [13]-[19] turns out to be a key enabling technology. It is widely known that STAP can adaptively adjust the two-dimensional space-time filter response in order to fully maximize output SINR, and thus provide better slow-moving target detection performance in strong clutter and jammer environment. As a classical reduced-dimension (RD) STAP method in conventional PA radar, JDL algorithm [14] transforms the receiving data into angle-Doppler domain, and implements adaptive processing in the selected joint domain, which reduces the number of training samples and computation burden. Considering that the original JDL method is not suitable for MIMO radar, we compare the STAP performance utilizing the BBM-JDL method [16]. The operation of discrete Fourier transform (DFT) is replaced by jointly transmit-receive beamforming with all the signals extracted by matched filter (MF) bank exploited. Nonadaptive performances are also compared and analysed based on conventional beamforming.

This paper is organized as follows: In Section 2 we formulate the generalized model of airborne radar. In Section 3, we present the formulation and analysis of STAP and nonadaptive processing, BBM-JDL method is also stated. Simulation results are presented in Section 4. Finally, we conclude this paper in Section 5.

2 Signal Model

In this section, we construct a generalized signal model for PA and MIMO radar systems with subarrays. Figure 1 illustrates an airborne radar system in which the platform travels along the positive *y*-direction at a speed of υ_p. The platform is assumed to locate over the *x*-*y* plane with a height of h. As shown in Figure 1, a side-looking uniform linear array (ULA) configuration is employed for transmitter and receiver. There are M transmitting elements with uniform space d_T and N receiving elements with uniform space d_R. The transmit and receive arrays are both linear and parallel, and each one contains a group of omnidirectional elements. Consequently, they share the same azimuth θ and elevation angle φ. The transmitting elements are evenly partitioned into K subarrays that are allowed to overlap. In this paper, we also assume that the transmitting waveforms meet the narrow-band condition, and λ be the operation wavelength. We also assume that T_r be the

pulse repetition interval (PRI), and one coherent processing interval (CPI) consists of L pulses. Let $\overline{\mathbf{s}}_k \in \mathbb{C}^{N_S \times 1}$, $k = 1, 2, \ldots, K$ be the length-N_s discrete version of the complex baseband waveform at the kth transmitting subarray in each PRI. Mutually orthogonal or non-coherent waveforms are employed at the transmitting end for MIMO radar while identical ones for PA. Thus the signal matrix can be denoted as $\overline{\mathbf{S}} = \left[\overline{\mathbf{s}}_1 \quad \overline{\mathbf{s}}_2 \quad \ldots \quad \overline{\mathbf{s}}_K\right] \in \mathbb{C}^{N_S \times K}$. In order to guarantee a fair comparison, we define the autocorrelation of each element in $\overline{\mathbf{S}}$ to be unitary. Thus the output signal matrix of the kth subarray can be expressed as

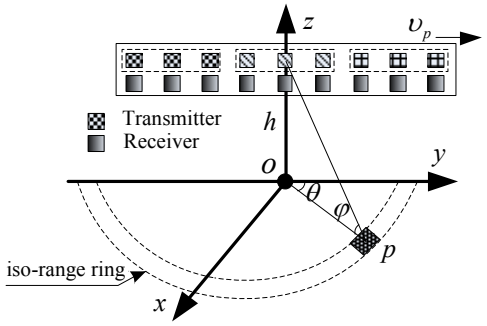

Figure 1 The geometry of MIMO STAP radar system

$$\mathbf{u}_k = \sqrt{\frac{M}{K}}\overline{\mathbf{s}}_k \overline{\mathbf{w}}_k^H \in \mathbb{C}^{N_S \times P}, \quad k = 1, 2, \ldots, K. \tag{1}$$

meaning that the total transmit energy of the kth subarray is equal to M/K. $\overline{\mathbf{w}}_k$ is the $P \times 1$ unit-norm beamforming weight vector with P being the number of elements in each subarray. The notation $(\bullet)^H$ means the conjugate transpose. Therefore, the echoes reflected from an iso-range ring for the lth pulse can be illustrated as

$$\begin{aligned} \mathbf{y}_l &= \int_0^{2\pi} \xi(\theta) e^{-j2\pi f_d(\theta)(l-1)} \sum_{k=0}^{K} \mathbf{u}_k \mathbf{a}_k(\theta) e^{-j2\pi(k-1)\psi_T} \mathbf{a}_R^T(\theta) \mathrm{d}\theta \in \mathbb{C}^{N_S \times N} \\ &= \int_0^{2\pi} \sqrt{\frac{M}{K}} \xi(\theta) e^{-j2\pi f_d(\theta)(l-1)} \sum_{k=0}^{K} \overline{\mathbf{s}}_k \overline{\mathbf{w}}_k^H \mathbf{a}_k(\theta) e^{-j2\pi(m-1)\psi_T} \mathbf{a}_R^T(\theta) \mathrm{d}\theta \end{aligned} \tag{2}$$

where $\xi(\theta)$ denotes the reflected coefficient and $f_d = 2\upsilon_p \cos\theta\cos\varphi T_r/\lambda$ denotes the normalized Doppler frequency. $\psi_T = 2\pi P d_T \cos\theta\cos\varphi/\lambda$ is the phase shift induced by the distance between adjacent subarrays which means that the distance between any two neighbour transmit phase centers is P times that of d_T. $\mathbf{a}_R(\theta)$ is the $N \times 1$ receive steering vector defined as

$$\mathbf{a}_R(\theta) = \left[1, e^{-j\psi_R}, \ldots, e^{-j(N-1)\psi_R}\right]^T \in \mathbb{C}^{N \times 1} \tag{3}$$

where $\psi_R = 2\pi d_R \cos\theta\cos\varphi/\lambda$ is the phase shift induced by the distance of the receiving element. The notation $(\bullet)^T$ means the matrix transpose. $\mathbf{a}_k(\theta)$ is the steering vector of the kth subarray. A way of simplifying the analysis is to select $\mathbf{a}_k(\theta)$ as

$$\mathbf{a}_k(\theta)=\left[1,e^{-j\psi_T/P},\ldots,e^{-j(P-1)\psi_T/P}\right]^T\in\mathbb{C}^{P\times 1}. \tag{4}$$

We define the transmit steering vector $\mathbf{a}_T(\theta)$ as

$$\mathbf{a}_T(\theta)=\left[1,e^{-j\psi_T},\ldots,e^{-j(K-1)\psi_T}\right]^T\in\mathbb{C}^{K\times 1}. \tag{5}$$

Define the coherent processing gain of the K subarrays as

$$\mathbf{C}_h(\theta)=\left[\overline{\mathbf{w}}_1^H\mathbf{a}_1(\theta)\quad\ldots\quad\overline{\mathbf{w}}_K^H\mathbf{a}_K(\theta)\right]^T\in\mathbb{C}^{K\times 1}. \tag{6}$$

By dividing the iso-range ring into N_c clutter patches in the cross-range direction, equation (6) can be denoted in the discrete form as

$$\mathbf{y}_l=\sum_{i=1}^{N_c}\sqrt{\frac{M}{K}}\xi(\theta_i)e^{-j2\pi f_d(\theta_i)(l-1)}\overline{\mathbf{S}}\left(\mathbf{C}_h(\theta_i)\odot\mathbf{a}_T(\theta_i)\right)\mathbf{a}_R^T(\theta_i) \tag{7}$$

with θ_i denoting the azimuth of the ith clutter patch. Matched filter bank should be employed at the receivers in order to get sufficient statistics. Hence the clutter echoes for the lth pulse can be compressed by the matched signal matrix $\overline{\mathbf{S}}$. With the operation of stacking the compressed data into a $KN\times 1$ vector columnwise, we get the expression of $\mathbf{c}_l$ as denoted in equation (8) where $\mathbf{R}_{\overline{\mathbf{S}}}=\overline{\mathbf{S}}^H\overline{\mathbf{S}}$ and the notation $\mathrm{Vec}(\bullet)$ means stacking operation.

$$\begin{aligned}\mathbf{c}_l&=\mathrm{Vec}\left(\overline{\mathbf{S}}^H\mathbf{y}_l\right)\in\mathbb{C}^{KN\times 1}\\&=\sum_{i=1}^{N_c}\sqrt{\frac{M}{K}}\xi(\theta_i)e^{-j2\pi f_d(\theta_i)(l-1)}\mathbf{a}_R(\theta_i)\otimes\left[\mathbf{R}_{\overline{\mathbf{S}}}\left(\mathbf{C}_h(\theta_i)\odot\mathbf{a}_T(\theta_i)\right)\right]\end{aligned} \tag{8}$$

Stacking $\mathbf{c}_l$ for all the pulses we obtain the $L\times KN$ matrix $\mathbf{C}=[\mathbf{c}_1,\mathbf{c}_2,\ldots,\mathbf{c}_L]\in\mathbb{C}^{KN\times L}$ as the clutter data i.e.

$$\mathbf{C}=\sum_{i=1}^{N_c}\sqrt{\frac{M}{K}}\xi(\theta_i)\mathbf{a}_R(\theta_i)\otimes\left[\mathbf{R}_{\overline{\mathbf{S}}}\left(\mathbf{C}_h(\theta_i)\odot\mathbf{a}_T(\theta_i)\right)\right]\mathbf{a}^T\left(f_d(\theta_i)\right). \tag{9}$$

$\mathbf{a}\left(f_d(\theta_i)\right)$ is the time domain steering vector which is denoted as

$$\mathbf{a}\left(f_d(\theta)\right)=\left[1,e^{-2\pi f_d(\theta)},\ldots,e^{-2\pi(L-1)f_d(\theta)}\right]^T. \tag{10}$$

Define $\mathbf{d}(\theta)\in\mathbb{C}^{KN\times L}$ as

$$\mathbf{d}(\theta)=\mathbf{a}_R(\theta)\otimes\left[\mathbf{R}_{\overline{\mathbf{S}}}\left(\mathbf{C}_h(\theta)\odot\mathbf{a}_T(\theta)\right)\right]\mathbf{a}^T\left(f_d(\theta)\right). \tag{11}$$

Thus equation (9) can be denoted as

$$\mathbf{C}=\sum_{i=1}^{N_c}\sqrt{\frac{M}{K}}\xi(\theta_i)\mathbf{d}(\theta_i). \tag{12}$$

Similarly, the echo data of a target located in the direction of θ_t can be modeled as

$$\mathbf{X}_t=\sqrt{\frac{M}{K}}\beta(\theta_t)\mathbf{d}(\theta_t) \tag{13}$$

with $\beta(\theta_t)$ denoting the reflected coefficient of the target in the direction of θ_t. Thus under the signal-absence hypothesis H_0, the receiving data matrix $\mathbf{X}$ can be expressed as

$$\mathbf{X} = \mathbf{C} + \mathbf{N}. \tag{14}$$

where $\mathrm{Vec}(\mathbf{N})$ is assumed as a complex Gaussian distribution vector with zero mean and covariance matrix $\sigma_n^2\mathbf{I}$. Note that $\mathbf{I}$ is an $LKN \times LKN$ identity matrix. Under the signal-presence hypothesis H_1, the receiving data matrix can be denoted as

$$\mathbf{X} = \mathbf{X}_t + \mathbf{C} + \mathbf{N}. \tag{15}$$

3 Performance of STAP and Nonadaptive Processing

In this section, we formulate the STAP and nonadaptive processing performance on the basis of the unified signal model aforementioned. Considering that the straight-forward application of JDL method is no longer valid for MIMO radar because of the extra filtered transmit DOFs. We use BBM-JDL method as the SATP technique. For the nonadaptive case, conventional nonadaptive beamforming technique is employed [12].

3.1 Performance of STAP with BBM-JDL

It is well known that JDL transforms the receive data set to angle-Doppler domain by a two-dimensional discrete Fourier transform (DFT) in PA radar. However, this is not efficient for MIMO radar due to the non-linear spatial phase of the data after matched filtering. Figure 2 and Figure 3 show two types of synthesized phases for MIMO radar with different parameters γ which is space ratio between transmit and receive element/subarray. It can be shown that the phases of both types are nonlinear with the shape of a broken line, which disables the use of DFT. Consequently, joint transmit-receive beamforming seems to be a suitable way to settle this problem.

Figure 4 illustrates the processing procedure of BBM-JDL processor. The receive data is transformed to beam space by joint transmit-receive Beamforming whose principle is depicted by the sub-frame on the right side. Both the transmit and receive steering vectors are jointly applied to the receive data after matched filtering. The KN dimensional filtered data should be processed in spatial domain to form beams in the direction of current scanning angle. Meanwhile, Doppler processing should be implemented according to the frequency of current joint domain. As illustrated in Figure 4, when searching the whole space that MIMO radar can illuminate, N_B joint beams and L Doppler bins are formed. Adaptive matched filter (AMF) bank is employed to implement the STAP in the localized processing region (LPR) with data set $\boldsymbol{\chi}_l, l = 1, \ldots, L$.

Assuming that the transmit antennas are well illuminating the direction of target and all elements of $\mathbf{C}_h$ are equal. The size of the LPR is selected to be $N_b \times N_l$ which means N_l Doppler bins and N_b beams are contained in the lth LPR. Thus the STAP based on the linearly constrained minimum variance (LCMV) criterion can be formulated as

$$\begin{cases} \min\limits_{w} \mathbf{w}^H \mathbf{R}_l \mathbf{w} \\ s.t.\ \mathbf{w}^H \mathrm{Vec}\left(\mathbf{S}_t^l\right) = 1 \end{cases} \tag{16}$$

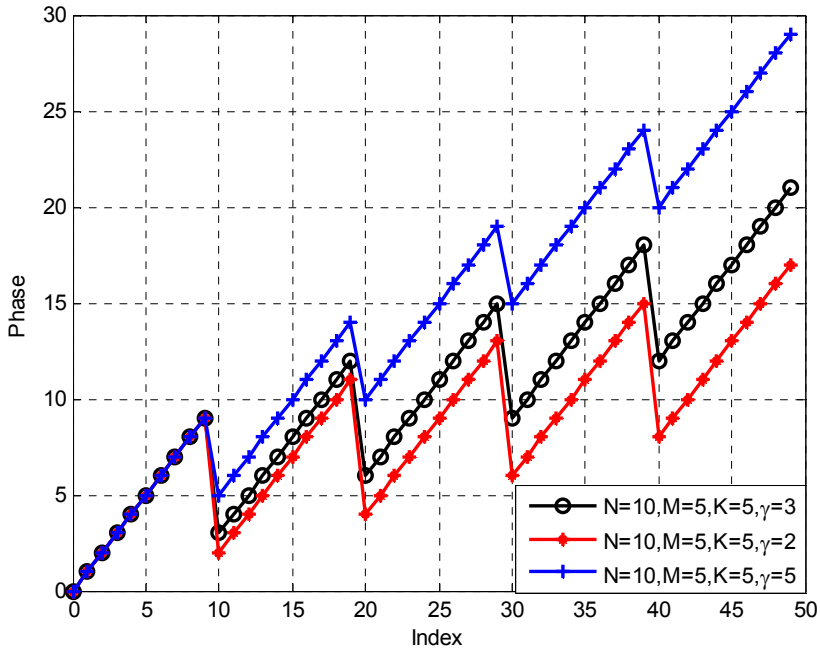

Figure 2 The synthesized receive-transmit phase

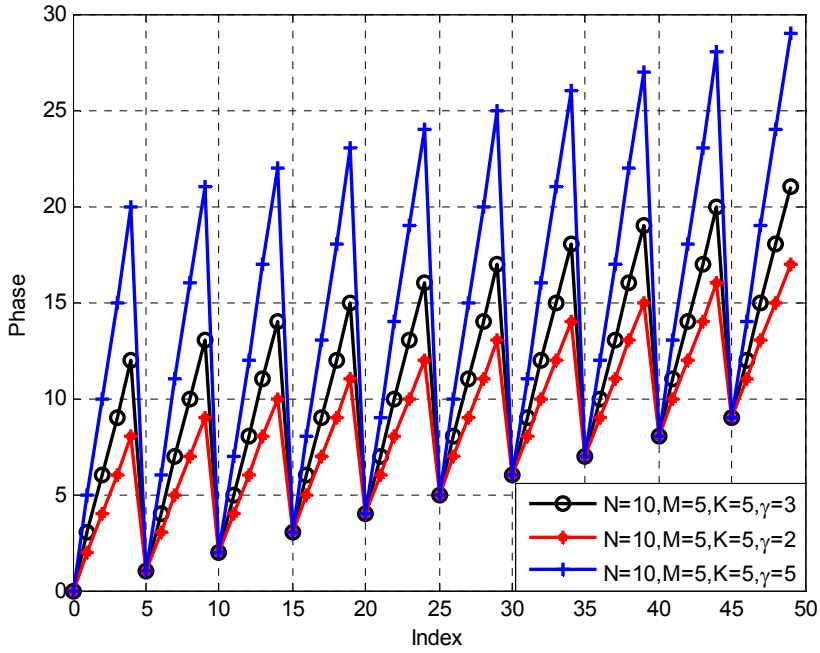

Figure 3 The synthesized transmit-receive phase

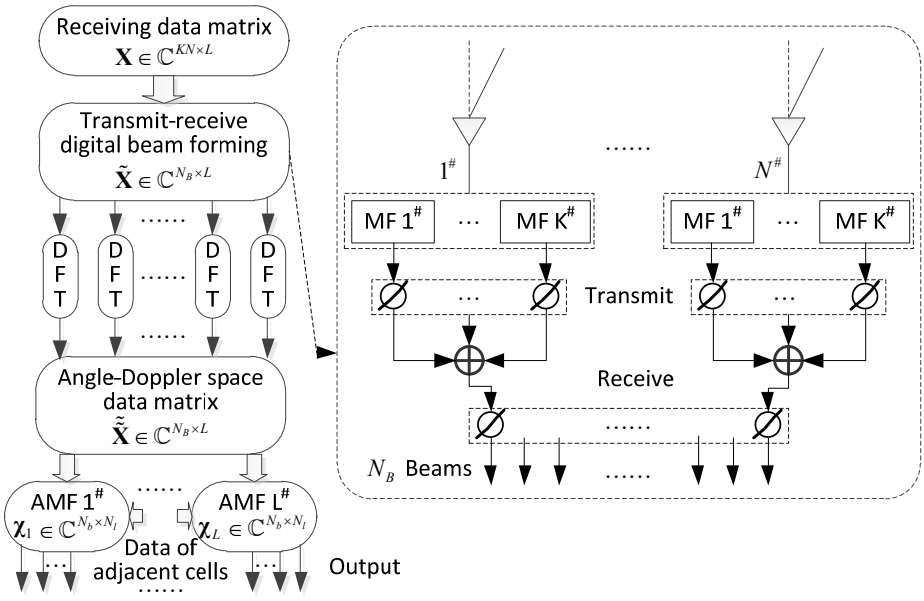

Figure 4 The block diagram of BBM-JDL method

where $\mathbf{w}$ is the weighted value, and $\mathbf{S}_t^l$ is the target steering matrix in angle-Doppler domain that has all its entries equal to zero except the target-mapping one which is LKN for the lth LPR . $\mathbf{R}_l \triangleq \mathrm{E}\left[\mathrm{Vec}\left(\boldsymbol{\chi}_l\right)\mathrm{Vec}^H\left(\boldsymbol{\chi}_l\right)\right]$ with $\mathrm{E}[\bullet]$ denoting the expectation and it can be estimated by the samples from the N_R neighbour range bins, i.e.

$$\hat{\mathbf{R}}_l = \frac{1}{N_R}\sum_{k=1}^{N_R}\mathrm{Vec}\left(\boldsymbol{\chi}_{l,k}\right)\mathrm{Vec}^H\left(\boldsymbol{\chi}_{l,k}\right). \tag{17}$$

The key objective of STAP is to maximize the output signal-to-interference-plus-noise ratio (SINR).

$$\mathrm{SINR}_{AP}^l = \frac{\dfrac{M}{K}\sigma_s^2\left|\mathbf{w}^H\mathrm{Vec}\left(\mathbf{S}_t^l\right)\right|^2}{\mathbf{w}^H\mathbf{R}_l\mathbf{w}} = \frac{\sigma_s^2L^2M^2N^2}{\mathbf{w}^H\mathbf{R}_l\mathbf{w}} \tag{18}$$

where $\sigma_s^2 = \mathrm{E}\left[\left|\beta\left(\theta_t\right)\right|^2\right]$.

It should be noted that PA with the $K=1$ case transmits identical waveform at each transmit element. Thus the narrow and high-gain beam is formed when beamforming is operated at the receiving end. However, this case does not work that way for MIMO radar. MIMO radar transmits low-gain wide beams because of the orthogonality of transmitting waveforms which cannot be stacked in homo-phase to synthesis high-gain narrow beam. Thus it is sensible to form multi-beams which cover the whole area.

One another important aspect to fix attention on is the differences in the noise power. The noise power after matched filtering for MIMO radar is K times that of PA which caused that the signal-to-noise ratio (SNR) of PA is K times that of MIMO radar. To make up for this loss, MIMO radar should possess K times integration time than PA in order to guarantee a same force.

Consequently, when adaptive matched filter is applied, clutter in the LPR is mitigated through a sidelobe canceller. Normally under the ideal condition, the residual clutter power can be very small if beams for cancelling are properly selected. Therefore, the output SINR will approach to the output SNR. So the SINR of PA and uniform MIMO will be equal.

3.2 Performance of Nonadaptive Processing

Conventional nonadaptive beamformer is known to be optimal in the sense that it provides the highest possible SNR gain in the case when a single source signal is observed in the background of white Gaussian noise. In this section, nonadaptive beamforming techniques are used for the angle-Doppler clutter of both systems with $\mathbf{w} = \mathrm{Vec}\left(\mathbf{d}\left(\theta_t\right)\right)$. The SINR of nonadaptive processing can be expressed as

$$\begin{aligned}\mathrm{SINR}_{NAP} &= \frac{\dfrac{M}{K}\sigma_s^2 \left\|\mathrm{Vec}\left(\mathbf{d}\left(\theta_t\right)\right)\right\|^4}{\mathrm{Vec}^H\left(\mathbf{d}\left(\theta_t\right)\right)\mathbf{R}\mathrm{Vec}\left(\mathbf{d}\left(\theta_t\right)\right)} \\ &= \frac{M/K\,\sigma_s^2 P_K^2 N^2 K^2 L^2}{M/K\sum_{i=1}^{N_c}\sigma_i^2\left|\mathbf{d}^H\left(\theta_s\right)\mathbf{d}\left(\theta_i\right)\right|^2 + \sigma_n^2 P_K NKL}\end{aligned} \tag{19}$$

where $\mathbf{R} \triangleq \mathrm{E}\left[\mathrm{Vec}\left(\mathbf{X}\right)\mathrm{Vec}^H\left(\mathbf{X}\right)\right]$, and $\sigma_i^2 = \mathrm{E}\left[\left|\xi\left(\theta_i\right)\right|^2\right]$ denotes the variance of the ith clutter patch.

It should be noted that the scenario of nonadaptive processing is indeed the lower bound of clutter mitigation. For the worst case when the spatial and Doppler frequency of a target is the same as that of clutter located in the clutter ridge, the performance of adaptive processing will decline to that of nonadaptive processing. Fortunately, the target can be separated from clutter in most cases, thus STAP can be easily applied to achieve higher detection performance.

As for nonadaptive processing technique, conventional beamforming is not capable of fully mitigating clutter, especially the mainlobe clutter, which results in wide clutter notch that means failing to achieve lower minimum detectable velocity (MDV). On the condition that MIMO and PA radar are on a basis of same SNR at the receiving end as mentioned above, obviously, MIMO radar can achieve higher Doppler resolution which increases the output SINR of the each Doppler bin. Consequently, MIMO radar is capable of detecting slower-moving target compared to its counterpart PA radar.

4 Simulation Results

In our simulation, $M = 16$, $N = 16$ antennas with half a wave length element space are selected. Clutter-to-noise ratio (CNR) is set to be 50 dB. The number of clutter patch N_c is set to be 1000. In the example, other basic parameters used are $\lambda = 0.69m$, $\upsilon_p = 107.8$ m/s, $h = 10$ km, $T_r = 1.6$ ms, and $\varphi = 0$ degree. Under the same coverage condition, we select $L_{PA} = 16$ and $L_{MIMO} = 64$.

In the first experiment as plotted in Figure 5, we evaluate the SINR performance of STAP against the target normalized Doppler frequency for PA and MIMO radar with subarrays that are uniform non-overlapped or fully overlapped. The target is located in the array looking direction of zero degree with $\mathrm{SNR} = \sigma_s^2 / \sigma_n^2 = 0\,\mathrm{dB}$. The corresponding parameters of the non-overlapped case are $K = 4$, $P = 4$ while the latter case chooses $K = 4$, $P = M - K + 1$. The sample covariance matrix is computed based on 100 data snapshots (i.e. 100 range bins). SINR performances are computed based on 200 independent simulation runs. In this simulation, the size of LPR is selected as 3×3. Adaptive output SNR performances are also shown.

Note that the SINR level of PA is nearly the same as that of MIMO radar with evenly divided subarrays. Indeed, the benefit produced by MIMO radar is the improved resolution shown by the narrower clutter notch. Because of efficient clutter mitigation, the output SINRs of these two systems nearly reach to the same level which is the output adaptive SNR. As illustrated in Figure 5, Overlapped MIMO radar has higher SINR at the cost of wide clutter notch which limits the detection of slow-moving target. Works aiming at this problem are under way.

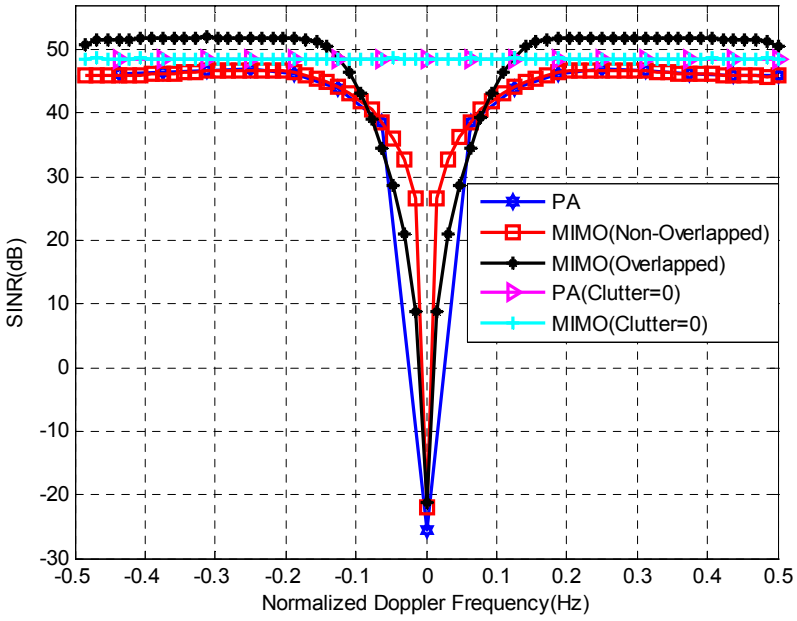

Figure 5 SINR performance of PA and MIMO

In the second experiment we evaluate the nonadaptive SINR performance using the same parameters as that in the first experiment. L is chose as 16 or 64. Figure 6 shows that PA and non-overlapped MIMO radar have the same performance when their integration time is equal. Performances of both systems become better when the integration time is increased. Under the same coverage condition, non-overlapped MIMO radar that possesses K times integration time of PA shows performance improvement at the level of about 10 dB, and this will enhance the capability of slow-

moving target detection. It is also shown that the fully overlapped MIMO radar possesses the best SINR performance compared to its counterparts in this case.

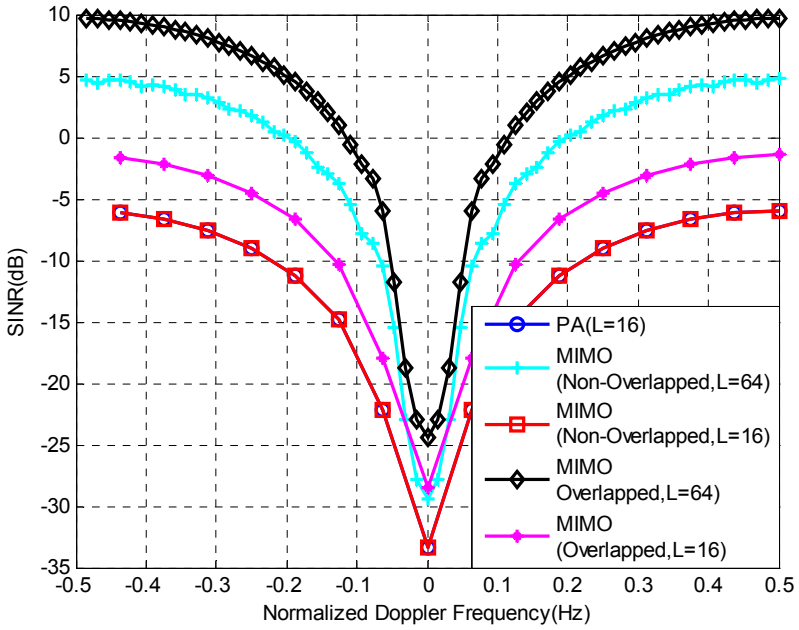

Figure 6 Nonadaptive SINR performance of PA and MIMO

6 Conclusion

In this paper, we developed a generalized signal model for airborne PA and MIMO radar with subarrays. Uniform non-overlapped and fully overlapped subarrys were considered. We focused on comparing the STAP and nonadaptive SINR performances of both radar systems. For the STAP case, the beamforming-based modified JDL method was employed as the STAP technique due to its less computation burden and efficient reduced-dimension adaptive processing capability. As for nonadaptive case, conventional beamforming method was selected. Simulation results showed that the STAP performances of PA and uniform non-overlapped MIMO radar are nearly the same as the output SNR because of the perfect clutter mitigation. The non-overlapped MIMO radar possesses a better performance which will enhance the slow-moving target detection under the same coverage condition. It is also shown that fully overlapped MIMO radar can achieve higher SINR performance in both cases, but it is weak in detecting slow-moving target when STAP is implemented.

Acknowledgements

The authors wish to acknowledge the collaborative funding support from the National Natural Science Foundation of China under Contract NSFC 61032010 and the Fundamental Research Funds for the Central Universities under Contact ZYGX2010YB007 and Contact ZYGX2010J015.

References

1. Bliss D. W. and Forsythe K. W., "Multiple-input multiple-output (MIMO) radar and imaging: degrees of freedom and resolution," in Proc. 37th IEEE Asilomar Conf. Signals, Systems, Computers, Nov. 2003, Vol .1, pp. 54-59.
2. Fishier E., Haimovich A., Blum R. S., Chizhik D., Cimini L., and Valenzuela R., "MIMO radar: An idea whose time has come," in Proc. IEEE Radar Conference, Apr. 2004, pp. 71-78.
3. Fishler E., Haimovich A., Blum R. S., Cimini L. J., Chizhik D., and Valenzuela R.A., "Performance of MIMO radar systems: Advantages of angular diversity," in Proc. 38th IEEE Asilomar Conference Signals, Systems, Computers, Nov. 2004, vol. 1, pp. 305–309.
4. Fishler E., Haimovich A., Blum R. S., Cimini L. J., Chizhik D., and Valenzuela R. A., "Spatial diversity in radars—models and detection performance," IEEE Transaction on Signal Processing, vol. 54, no. 3, pp. 823–837, Mar. 2007.
5. Forsythe K. W., Bliss D. W., and Fawcett G. S., "Multiple-input multiple-output (MIMO) radar performance issues," in Proc. 38th IEEE Asilomar Conference Signals, Systems, Computers, Nov. 2004, pp. 310–315.
6. Fuhrmann D. R. and Antonio G. S., "Transmit beamforming for MIMO radar systems using partial signal correlation," in Proc. 38th IEEE Asilomar Conference Signals, Systems, Computers, Nov. 2004, pp. 295–299.
7. Antonio G. S. and Fuhrmann D. R., "Beampattern synthesis for wideband MIMO radar systems," Proc. 1st IEEE Int. Workshop Computational Advances in Multi-Sensor Adaptive Processing, pp. 105–108, Dec. 2005.
8. Forsythe K. W. and Bliss D. W., "Waveform correlation and optimization issues for MIMO radar," in Proc. 39th IEEE Asilomar Conf. Signals, Systems, Computers, Nov. 2005, pp. 1306–1310.
9. Li J. and Stoica P., "MIMO radar with collocated Antennas," IEEE Signal Processing, Magzine, vol. 24, no. 9, pp. 106-114, Sep. 2007.
10. Bergin J., McNeil S., Fomundam L., and Zulch P., "MIMO phased-array for SMTI radar," in Proc. IEEE Aerospace Conference, Big Sky, MT, Mar. 2008, pp. 1-7.
11. Fuhrmann D., Browning J. P. and Rangaswamy M., "Signal strategies for the hybrid MIMO phased-array radar," IEEE Selected Topics Journal on Signal Process., vol. 4, no. 1, pp. 66-78, Feb. 2010.
12. Hassanien A., Vorobyov S. A., "Phased-MIMO radar: a tradeoff between phased-array and MIMO radars," IEEE Transaction on Signal Processing, vol. 58, no. 6, pp. 3137-3151, Jun. 2010.
13. Melvin W. L., "A STAP overview," IEEE Aerospace and Electronic System Magzine, vol. 19, no. 1, pp. 19-35, Jan. 2004.
14. Wang H. and Cai L., "On adaptive spatial-temporal processing for airborne radar Systems," IEEE Transaction on Aerospace and Electronic System, vol. 30, no. 3 pp. 660-670, Jul. 1994.
15. Chen C. Y. and Vaidyanathan P. P., "MIMO radar space time adaptive processing using prolate spheroidal wave functions," IEEE Trans. on Signal Process., Vol. 56, pp. 623-635, Feb. 2007.
16. Li Y. Z., He Z. S., Liu H. M., Li J., "A new STAP method for MIMO radar based on joint digital beam forming and joint domain localized processing," in the 2011 CIE International Conference on Radar, vol. II, pp. 1107-1110, Oct. 2011.
17. Ward J., Space–time adaptive processing for airborne radar, Lincoln Laboratory, Lexington, MA, Tech. Rep. 1015, Dec. 1994.
18. Guerci J. R., Space–Time Adaptive Processing. Norwood, MA: Artech House, 2003.
19. Klemm R., Principles of Space–Time Adaptive Processing. London, U.K.: IEE, 2002.
20. H. L. Van Trees, Optimum Array Processing: Part IV of Detection Estimation and Modulation Theory. New York: Wiley Interscience, 2002.